J. agric. Engng Res. (1977) **22**, 213–228

Soil Failure with Narrow Tines

R. J. GODWIN*; G. SPOOR*

A force prediction model has been developed for tines of a wide range of working depth/width ratios. The soil worked by the tines is assumed to obey the Mohr–Coulomb failure criterion. The predictions show useful agreement with experimental data for the horizontal force components in two soil conditions with high angles of shearing resistance. A method is proposed for estimating the critical depth of a tine, the depth below which the soil failure mechanism changes.

1. Introduction

Mathematical solutions for calculating forces are available for the two-dimensional soil failure situation with wide tines (blades), Osman,[1] Siemens and Weber,[2] Hettiaratchi *et al.*,[3] and for the three-dimensional case with narrow tines, Payne,[4] O'Callaghan and Farrelly,[5] Hettiaratchi and Reece.[6] The experimental verification of the narrow tine theories has been limited to tines whose working depth/width ratios, termed aspect ratios, are approximately 6 or less. Payne[4] suggested that the poor prediction for very narrow tines, i.e. high aspect ratios, was due to insufficient strain in the soil to cause failure. The soil failure patterns modelled in the earlier tine theories include the actual observed failure surface boundaries,[4] and simplified patterns involving both vertical and horizontal deformations.[5,6]

Both Zelenin[7] and Kostritsyn[8] observed a change in the soil failure mechanism at depth with very narrow tines. Above a certain critical depth, the soil was displaced forwards, sideways and upwards, and below it no upward movement occurred. For vertical tines, Kostritsyn[8] found that the critical depth occurred at an aspect ratio of approximately 7, whereas studies with sand in a glass-sided box by Miller,[9] showed the transition to be at aspect ratios of 12–14. O'Callaghan and McCullen[10] in their narrow tine theory considered the critical depth to be at an aspect ratio of 0·6 for vertical tines increasing to 2·7 for 45° rake angle tines.

This paper proposes a mathematical model which will estimate the forces and the position of the critical depth for a wide range of tine aspect ratios.

2. Soil failure pattern with narrow tines

Studies were carried out using a glass-sided box to observe the soil failure pattern in the vertical plane containing the centre line of the tine. Rigid tines of different width and rake angle, whilst firmly held against the sheet of glass, were pulled through a compact sandy loam soil until one soil shear plane had distinctly formed. The glass was assumed to be the axis of symmetry of the tine in the direction of travel. The effective tine width was therefore twice the actual tine width. The distance ahead of the tine at which the distinct shear plane broke the surface was defined as the forward rupture distance, f (see *Fig. 1*).

A compacted soil wedge was observed on the front of each tine at all tine widths and rake angles tested. With tines of small aspect ratio, the soil ahead of the wedge moved forwards and upwards over the entire working depth, with a distinct shear plane being developed from the tine base (crescent failure). As the tine aspect ratio increased, the soil below a certain depth (critical depth) appeared to move forwards only with no distinct shear plane being formed (lateral failure). Crescent failure occurred above this depth, with the distinct shear plane developing from the critical depth (*Fig. 1*). A decrease in the tine rake angle caused an increase in the critical

*National College of Agricultural Engineering, Silsoe, Bedford
Received 23 July 1976; accepted in revised form 4 January 1977

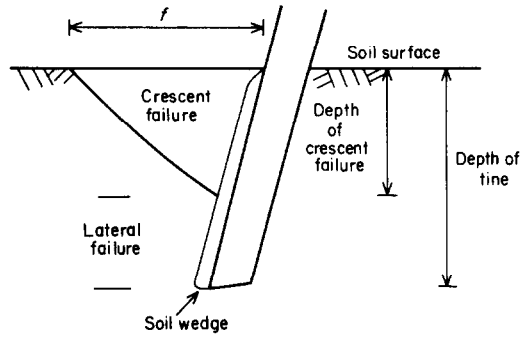

Fig. 1. Soil failure pattern

depth for a fixed tine aspect ratio. The results of these observations are plotted in a dimensionless manner in *Fig. 2*, where the crescent aspect ratio (depth of crescent failure/tine width) is plotted against the aspect ratio for different rake angle tines. The results obtained by Miller[9] and the values suggested by Kostritsyn[8] are shown to be in close agreement.

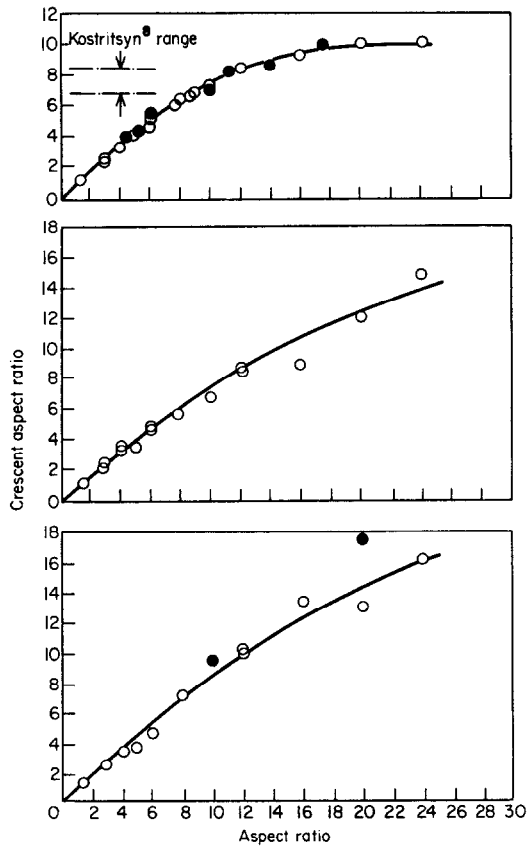

Fig. 2. Relationship between crescent aspect ratio and aspect ratio for 90° rake angle tines (top), 67·5° rake angle tines (middle) and 45° rake angle tines (bottom). Solid points from Miller[9]

A plot of the ratio forward rupture distance/tine width against tine aspect ratio for three rake angles is shown in *Fig. 3* (left). Where comparisons can be made, i.e. at small aspect ratios, the values obtained are in close agreement with those of Payne[4] and Payne and Tanner.[11] The non-linear nature of the relationship is due to the effect of changes in the depth of crescent failure. Where the results are plotted in terms of the crescent aspect ratio, *Fig. 3* (right) the relationship is linear.

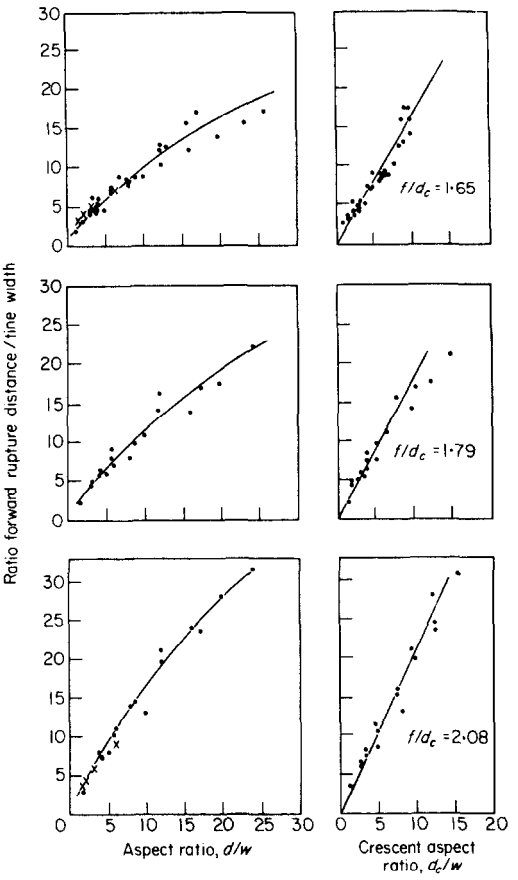

Fig. 3. Left: relationship between the ratio of forward rupture distance/tine width and aspect ratio for 90° rake angle tines (top), 67·5° rake angle tines (middle) and 45° rake angle tines (bottom). Crosses from Payne [4] and Payne and Tanner.[11] Right: relationship between the ratio of forward rupture distance/tine width and crescent aspect ratio for 90° rake angle tines (top) 67·5° rake angle tines (middle) and 45° rake angle tines (bottom)

Measurements of the rupture distance made in the glass-sided box were not significantly different at the 95% confidence level from those made in a soil bin filled with similar soil. This indicated that soil/glass friction had not significantly affected the failure pattern.

The soil failure mechanism below the critical depth was considered to be purely two-dimensional in a horizontal plane. The nature of the failure was examined in detail by pushing horizontally, vertical tines of different widths into soil beneath a horizontal sheet of laminated glass. Plan photographs at 0·5 s exposure, were taken through the glass to determine the soil particle trajectories. The photographs, illustrated by *Fig. 4*, showed the particle trajectory to have forward,

sideways and backward components. Although it was possible to make only subjective assessments, it was concluded that this type of soil deformation pattern was similar to that postulated by Jaky[12] and Meyerhof[13] for deep footings.

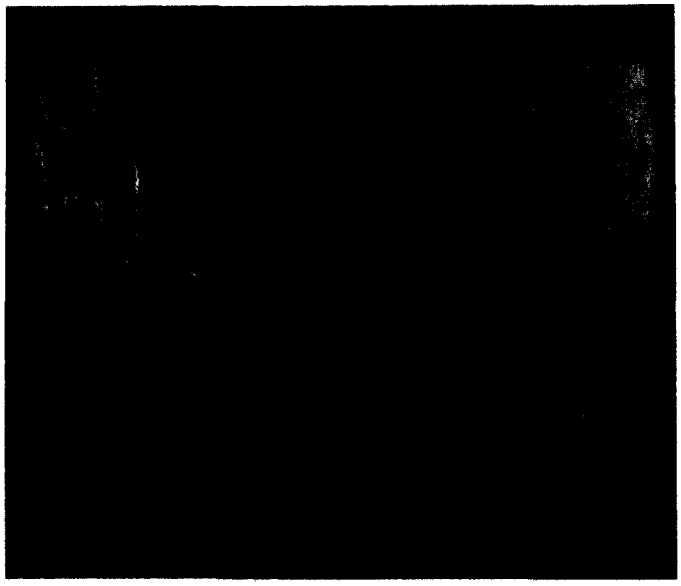

Fig. 4. Horizontal soil failure

3. Force prediction model

In section 2 it was shown that two failure mechanisms can be identified:

(a) an upper failure zone where the displaced soil has forward, sideways and upward components, termed crescent failure;

(b) a lower failure zone where the displaced soil has components both in the direction of travel and sideways, termed lateral failure.

This is shown diagrammatically in *Fig. 5* (left). For tines with small aspect ratios, the failure mechanism will be wholly of the crescent type. For tines with very large aspect ratios, much of the soil failure will be of the lateral type.

The prediction model is based upon the assumption that the soil worked by the tines obeys the Mohr–Coulomb failure criterion. It is assumed the soil is homogenous and isotropic and that inertia forces can be neglected.

3.1. *Crescent failure*

A simple passive failure is considered to occur in the crescent failure area. The magnitude of the resultant passive force can be rapidly estimated from the equation for plane failure in front of wide cutting blades, given by Hettiaratchi *et al.*[3,14]

$$P = \gamma z^2 N_\gamma + czN_c + c_a zN_a + qzN_q. \qquad \ldots(1)$$

The N factors in each of the terms are dimensionless numbers whose magnitude is dependent upon the magnitude of α, ϕ and δ. Their value has been determined using a numerical analysis presented by Sokolovski.[15]

The crescent itself comprises a linear section immediately ahead of the tine width equal to the tine width, flanked by two curved sections of constant radius, see *Fig. 5* (right).

The passive force per unit width of the linear portion which acts at an angle δ to the normal to the tine force can be determined using Eqn (1).

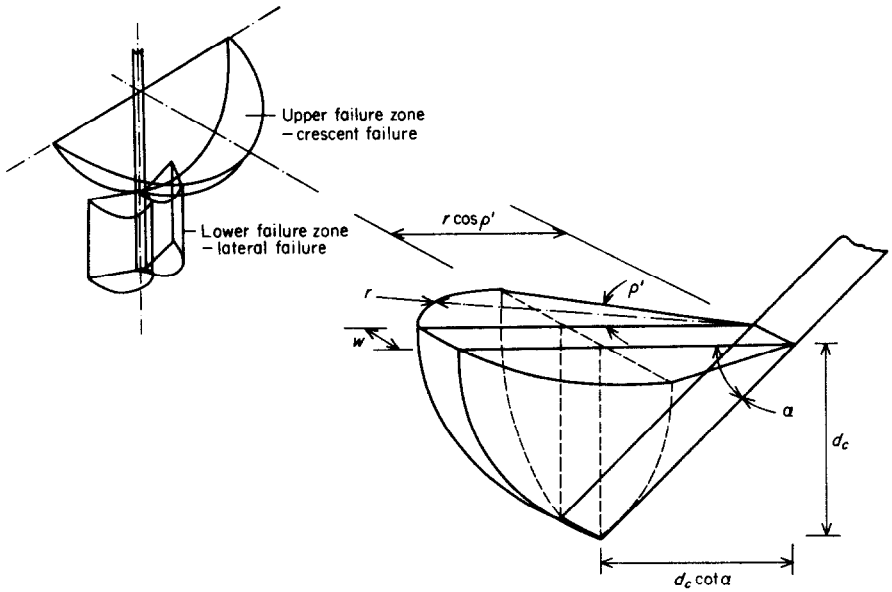

Fig. 5. Left: conceptual mechanism of soil failure. Right: crescent geometry

NOTATION

c	cohesion
c_a	soil-interface adhesion
d	depth of tine
d_c	critical depth
f	forward rupture distance
m	rupture distance ratio
p_0	geostatic stress
q	surcharge pressure
q'	stress on tine face, at depths greater than the critical depth
r	crescent radius $= f$
w	width of tine
z	depth
D	total horizontal force on the tine
F	$\gamma d_c^2 N_\gamma + c d_c N_c + q d_c N_q$
H	horizontal force component of radial zone
H_T	horizontal force component of the crescent failure
K_0	ratio of horizontal to vertical stress on the soil at rest
N	dimensionless number
Suffixes to N: γ = gravitational, c = cohesive, a = adhesive, q = surcharge (these can be found in References (3) and (14); in the latter reference they are reported as K values†)	
N'	dimensionless number. *Suffixes:* q = gravitational, c = cohesive
dP	passive force of crescent element acting at ρ to the direction of travel
Q	force on tine face, at depths greater than the critical depth
V	vertical force component of radial zone
V_T	vertical force component
α	rake angle from the forward horizontal
δ	angle of soil-interface friction
γ	soil bulk density
β, η, θ	see *Fig. 7*
ϕ	angle of shearing resistance
ρ	angle of crescent element from the direction of travel
ρ'	maximum angular limit of ρ
ψ	$45° + \phi/2$

The following approximation permits the complex radial failure to be analysed using existing two-dimensional theory. The angle ρ' between the direction of travel and the termination of the curved section of the crescent is given by:

$$\rho' = \cos^{-1}\left(\frac{\cot \alpha}{m}\right) \qquad \ldots(2)$$

where

$$m = r/d_c. \qquad \ldots(3)$$

The passive force dP necessary to cause shear of a volumetric element contained in the sector dρ radiating from the edges of the tine force to the crescent boundary, see *Fig. 6* (upper) is given by Eqn (4). This force acts at an angle ρ to the direction of travel and at an angle δ to the normal to the tine face, see *Fig. 6* (lower).

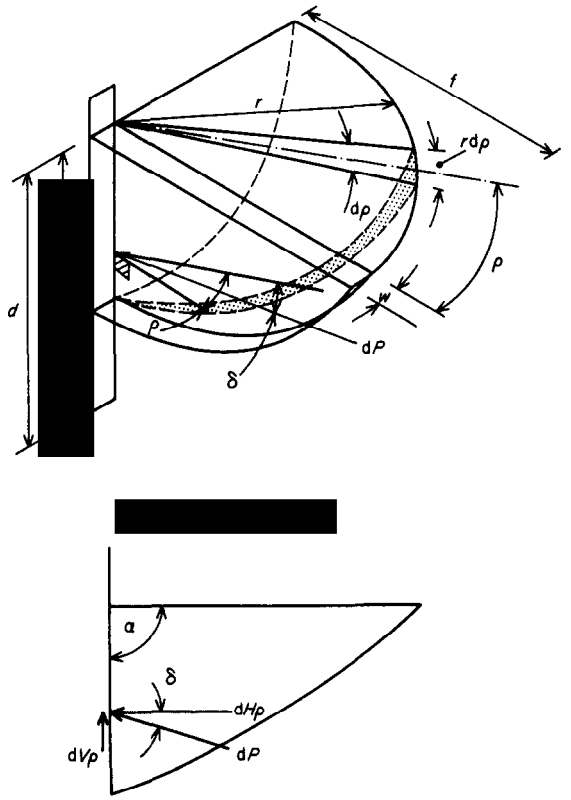

Fig. 6. Crescent soil failure mechanism

$$\mathrm{d}P = (\gamma d_c^2 N_\gamma + c d_c N_c + q d_c N_q)\frac{r\mathrm{d}\rho}{2}, \qquad \ldots(4)$$

It is assumed that $r\mathrm{d}\rho/2$ is the effective width of the element. In practice, $r\mathrm{d}\rho/2$ may be an under- or over-estimate of the mean width of the shear plane depending whether the shear plane is convex or concave. The adhesive component in the radial zone is neglected because the tine width at the tine is infinitely small. It is assumed, for all rake angles, that the element is vertical and radiates at an angle ρ to the direction of travel at all depths (this is the case for the 90° rake angle tines). Allowing F to represent the terms enclosed in the brackets in Eqn (4), the horizontal and vertical force components of dP are given by:

$$\mathrm{d}H\rho = F\frac{r\mathrm{d}\rho}{2}\sin(\alpha+\delta), \qquad \ldots(5)$$

$$dV\rho = -F\frac{r d\rho}{2}\cos(a+\delta). \quad ...(6)$$

Upward forces are considered positive. The component of $dH\rho$ (Eqn (5)) in the direction of travel is:

$$dH = F\frac{r}{2}\sin(a+\delta)\cos\rho d\rho \quad ...(7)$$

Substituting for r and integrating Eqn (7) between the limits $\rho = 0$ and $\rho = \rho'$ gives the horizontal force component for one curved crescent section:

$$H = F\frac{md_c}{2}\sin\left[\cos^{-1}\left(\frac{\cot a}{m}\right)\right]\sin(a+\delta). \quad ...(8)$$

The total horizontal force component, in the direction of travel for the linear and two curved sections, including interface adhesion above the critical depth is given by:

$$H_T = [\gamma d_c^2 N_\gamma + cd_c N_c + c_a d_c N_a + qd_c N_q]w\sin(a+\delta) + 2H + c_a w d_c \cos a \quad ...(9)$$

which becomes

$$H_T = [\gamma d_c^2 N_\gamma + cd_c N_c + qd_c N_q]\left[w + md_c \sin(\cos^{-1}\left(\frac{\cot a}{m}\right))\right]\sin(a+\delta) + c_a w d_c (N_a \sin(a+\delta) + \cos a) \quad ...(10)$$

Substituting for r and integrating Eqn (6) between the limits $\rho = 0$ and $\rho = \rho'$ gives the vertical component for one curved crescent section:

$$V = -F\frac{md_c}{2}\cos^{-1}\left[\frac{\cot a}{m}\right]\frac{\pi}{180}\cos(a+\delta). \quad ...(11)$$

The total vertical force component in the direction of travel for the linear and two curved sections, including interface adhesion above the critical depth is given by:

$$V_T = -[\gamma d_c^2 N_\gamma + cd_c N_c + cad_c N_a + qd_c N_q]w\cos(a+\delta) + 2V + c_a w d_c \sin a \quad ...(12)$$

which becomes

$$V_T = -[\gamma d_c^2 N_\delta + cd_c N_c + qd_c N_q]\left[w + m\, d_c \cos^{-1}\left[\frac{\cot a}{m}\right]\frac{\pi}{180}\right]\cos(a+\delta) - c_a w d_c [N_a \cos(a+\delta) - \sin a]. \quad ...(13)$$

3.2. *Lateral failure*

The soil below the critical depth is considered to fail in a two-dimensional manner in a horizontal plane regardless of the tine rake angle, *Fig. 7* (top). This type of failure is similar to that of a deep narrow footing orientated at 90° to the normally accepted direction of application. The logarithmic spiral analysis is used in this model because Scott[16] has shown that this technique developed by Meyerhof[13] deviates only marginally from the more complex numerical solution of Sokolovski.[15]

The logarithmic spiral boundaries shown in *Fig. 7* (bottom), extend beyond the plane containing the face of the tine. Meyerhof[13] has shown that the resultant force on a footing is relatively insensitive to the degree of mobilization of shear stresses along the face AE; therefore, shear stresses on this face are neglected. To meet this condition the angle η must be $(45°-\phi/2)$. In the case of a true footing, the angle β between the face of the footing and the face AE is a function of the footing depth. For the narrow tine case it would appear logical that the angle β should

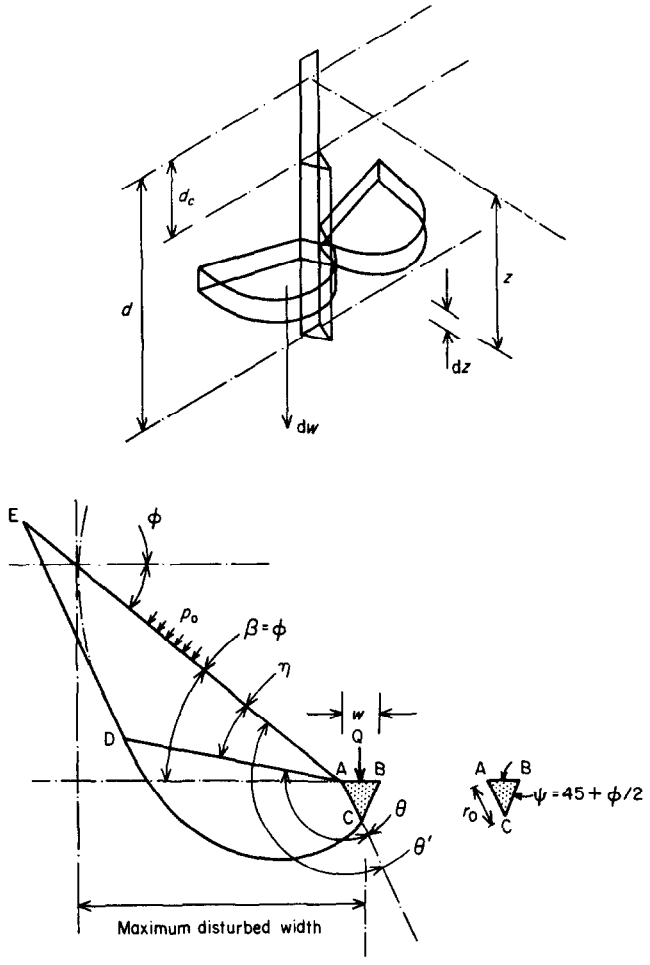

Fig. 7. Lateral soil failure mechanism

describe the position of the radius vector of the spiral with the maximum component in the lateral direction. In this case, the failure mechanism extends through undisturbed soil only, and the angle β must be equal to the angle of shearing resistance ϕ. Following practical observations and the theoretical derivations developed by Hettiaratchi and Reece[6] the roughness of the tine face is neglected and the angle between the face and the wedge side, ψ, is therefore considered to be $(45+\phi/2)$.

Since the weight of soil in the element dz acts parallel to the vertical axis of the tine, and the frictional force along the spiral surface CD passes through the spiral pole, neither have a moment resisting the passage of the tine. The only gravitational effect is due to the geostatic stress acting normal to the face AE. The magnitude of this geostatic stress is:

$$p_0 = K_0 \gamma z \qquad \ldots(14)$$

where K_0 is the ratio of the horizontal to vertical stress on the soil at rest, and $K_0 = (1-\sin\phi)$ (Lambe and Whitman[17]).

The resultant stress on the tine can be obtained from the Meyerhof[13] solution where

$$q' = cN_c' + p_0 N_q'. \qquad \ldots(15)$$

The total force Q on the tine face below the critical depth is therefore given by the integration of Eqn (15) between the limits of the critical depth d_c and the total working depth d:

$$Q = wcN_c'(d-d_c)+0{\cdot}5\,K_0\gamma wN_q'(d^2-d_c^2). \qquad ...(16)$$

The values of the factors N_c and N_q can be determined from the expressions below, Meyerhoff,[13] or from *Fig. 8:*

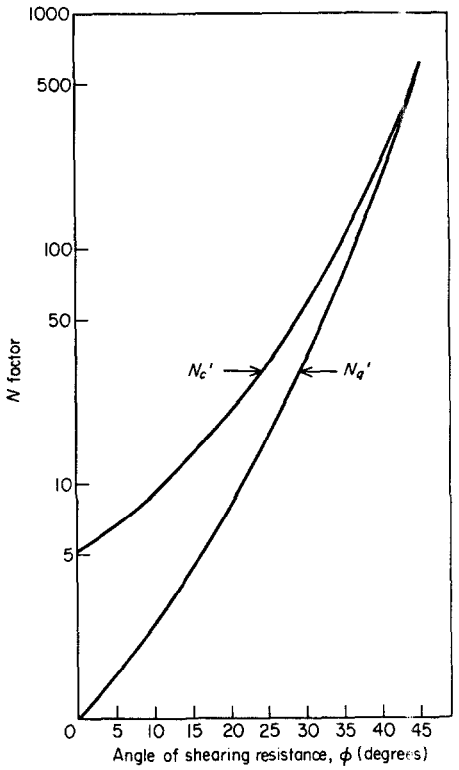

Fig. 8. Dimensionless N factors for lateral soil failure

$$N_c' = \cot\phi\left[\frac{(1+\sin\phi)e^{2\theta\tan\phi}}{(1-\sin\phi\sin(2\eta+\phi))}-1\right], \qquad ...(17)$$

$$N_q' = \frac{(1+\sin\phi)\,e^{2\theta\tan\phi}}{1-\sin\phi\sin(2\eta+\phi)}. \qquad ...(18)$$

The horizontal force component of the soil reaction on the tine, D, is given by the following equation:

$$D = H_T+Q. \qquad ...(19)$$

The substitution of Eqns (10) and (16) into Eqn (19) allows the horizontal force component to be evaluated. The vertical force component is evaluated from Eqn (13).

3.3. *Model evaluation*

Fig. 9 allows a comparison to be made between the predicted and measured forces for a range of 90° rake angle tines, working at two depths, 165 and 115 mm. The soil strength parameters were as follows:

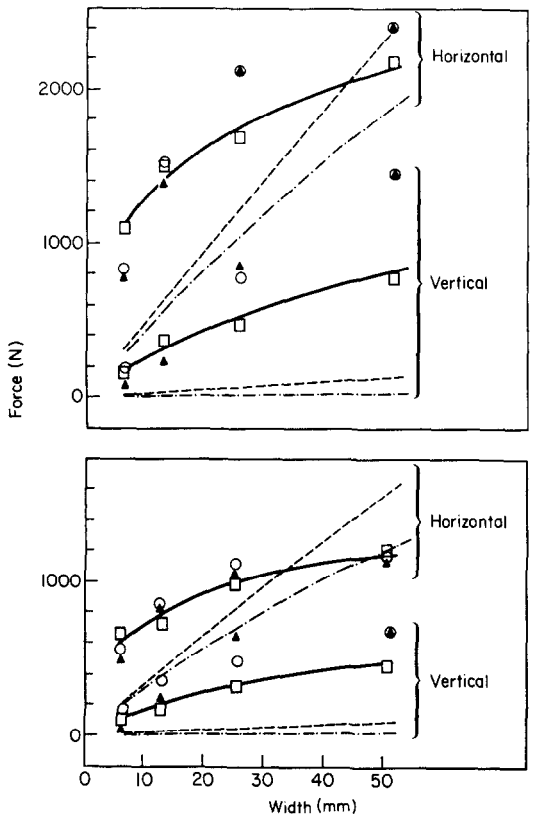

Fig. 9. Comparison between predicted and measured forces on 90° rake angle tines at two depths of operation, 165 mm (upper) and 115 mm (lower). ○, Values calculated using the depth of crescent failure given in Fig. 2; ▲, Values calculated using the critical depths given by Eqn (20); — — — — — values calculated using the Hettiaratchi–Reece[6] model; — · — · —, values calculated using the O'Callaghan-Farrelly[5] model; — □ —, experimental data

$$\phi = 37{\cdot}5°,\ c = 4{\cdot}6\ \text{kN/m}^2,\ \delta = 22°,$$
$$c_a = 0,\ \gamma = 1500\ \text{kg/m}^3.$$

The critical depth was determined from glass-sided box studies.

Predictions using the Hettiaratchi and Reece[6] and O'Callaghan and Farrelly[5] theories are also included. Their predictions for the horizontal force acting on the wider tines is satisfactory. Deviation occurs, however, as the tines get narrower and the contribution to the total force from lateral failure below the critical depth increases.

Fig. 9 shows that whilst the magnitude of the horizontal force is predicted relatively well, the magnitude of the vertical force is over-estimated for the wider tines. The reason for this inconsistency is that in order to simplify the model it was assumed that the crescent is of a constant radius equal to the forward rupture distance. However, the soil bin tests and the work of Payne and Tanner[11] suggest that the forward rupture distance is greater than the sideways rupture distance. For horizontal force predictions the effect of changing the radius is small, as the component of dP in the direction of travel for values of ρ approaching 90° is small. For vertical force predictions the total vertical force on the tine is independent of the magnitude of ρ, therefore the effect of an over-estimate of dP for values of ρ approaching 90° is reflected in the magnitude of the vertical force.

4. Estimation of the critical depth

It was demonstrated in section 3 that with a knowledge of the critical depth for a particular tine in a given soil, useful estimates can be made of the horizontal and vertical force components acting on narrow tines.

In practice the position of the critical depth is unknown and unless this can be found using an alternative technique to a glass-sided box, the theory proposed is of limited practical value.

In the proposed theory, the soil can deform by either crescent failure, lateral failure, or a combination of both. If it is assumed that the soil ahead of the tine will fail in such a way that the horizontal force will be a minimum, then a numerical procedure can be used to determine the position of the critical depth. This is an extension of classical soil mechanics procedures, Terzaghi,[18] where the magnitude of the passive force is determined by selecting the failure boundary that gives the smallest passive force. The critical depth can be determined using either of the procedures proposed below:

(a) iterative, where the magnitude of the horizontal force is determined for different assumed values of the critical depth;
(b) differentiation, where the horizontal force function, Eqn (19) is differentiated with respect to the critical depth and equated to zero.

The resulting function is in the form of a quadratic where the critical depth is in the positive root of Eqn (20):

$$d_c = \frac{-b \pm \sqrt{b^2-4ac'}}{2a}, \qquad \ldots(20)$$

where

$$a = 3\gamma N_\gamma \sin(\alpha+\delta)m \sin\left(\cos^{-1}\left(\frac{\cot\alpha}{m}\right)\right) \qquad \ldots(21)$$

$$b = 2(cN_c+qN_q)m \sin\left(\cos^{-1}\left(\frac{\cot\alpha}{m}\right)\right)\sin(\alpha+\delta) + 2\gamma N_\gamma \sin(\alpha+\delta)w-(1-\sin\phi)\gamma wN_q', \qquad \ldots(22)$$

$$c' = (cN_c+c_aN_a+qN_q)\sin(\alpha+\delta)w+c_a\omega\cos\alpha-wcN_c'. \qquad \ldots(23)$$

The results from the iterative procedure are illustrated graphically in *Fig. 10* for a range of tines. These tines were working at constant depth in a compact soil condition, similar to that described in section 3, and in an uncompacted condition where the soil properties were as follows:

$$\phi = 34°,\ c = 0,\ \delta = 22°,\ c_a = 0,\ \gamma = 1100\ \text{kg/m}^3.$$

The estimated draught values are plotted against the corresponding assumed values of the critical depth.

Comparing the critical depth positions, corresponding to the minimum horizontal force, for both soils, it can be seen that the critical depth is much closer to the surface in the uncompacted soil *Fig. 10* (top), than in the compacted soil, *Fig. 10* (middle and bottom). The critical depth is very sensitive to changes in both soil density and angle of shearing resistance. The latter is illustrated in *Fig. 10* (middle) where for the four different widths of the 90° rake angle tines, the critical depths, calculated using Eqn (20), for $\phi = 35°$ and $\phi = 40°$ are shown in addition to that for $\phi = 37{\cdot}5°$. This range of ϕ values was chosen because it represents the 95% confidence limits for the measured ϕ. The critical depth values observed in the glass-sided box are also shown. The minimizing technique appears to predict the critical depth, for the compact soil condition, to within ± 30 mm. Whilst this deviation may be unacceptable for relatively shallow working tines, it should be sufficiently accurate for tines working at depths of 200 mm or more.

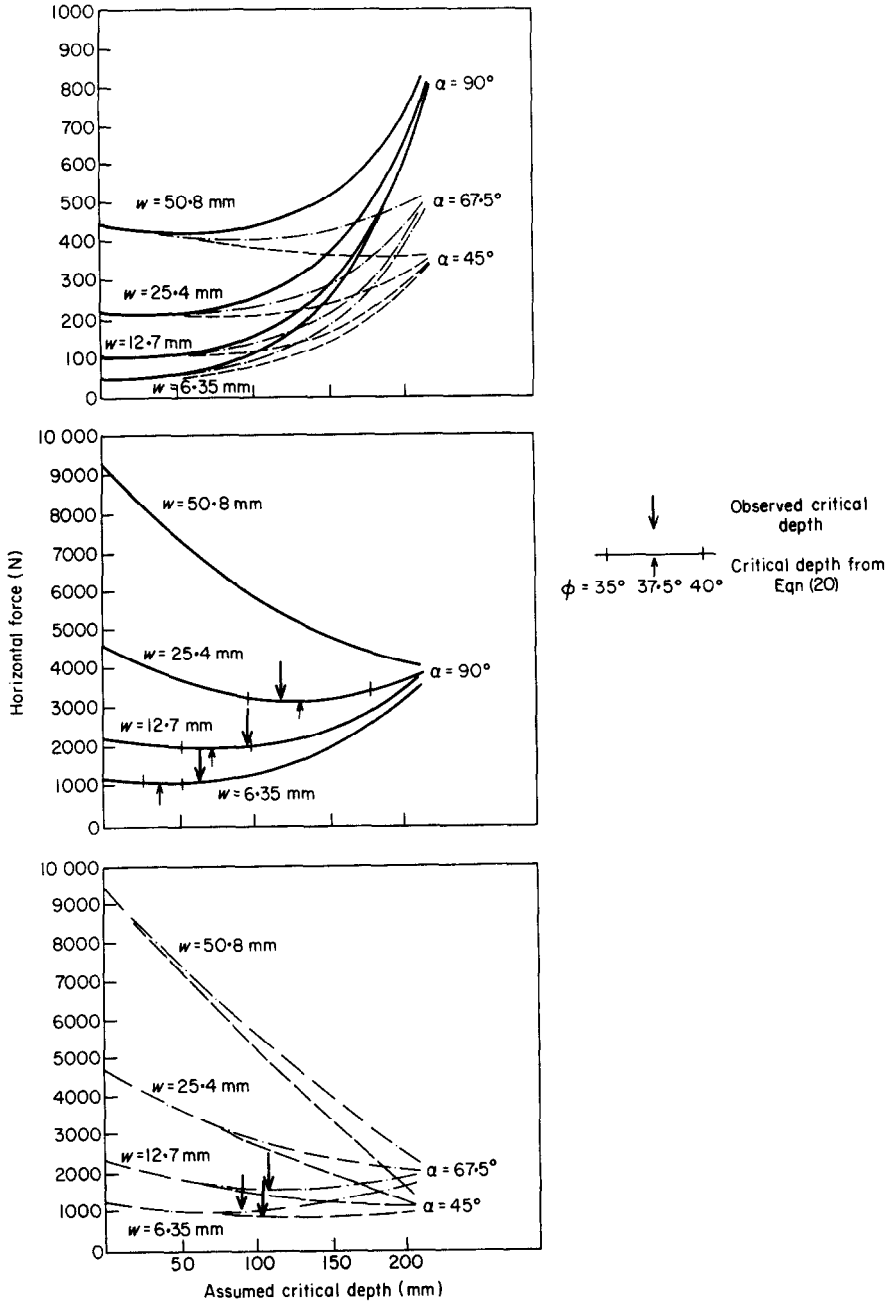

Fig. 10. Relationship between the horizontal force and the position of the assumed critical depth. Top: 90°, 67·5° and 45° rake angles, uncompacted soil. Middle: 90° rake angle, compacted soil. Lower: 67·5° and 45° rake angles, compact soil

The tine force predictions made using the critical depth values estimated both from the minimizing technique and the glass-sided box can be compared for the compact soil condition in *Fig. 9*. They show good agreement.

5. Calculation of forces

To estimate the forces acting on narrow tines using Eqns (13) and (19), information on the tine geometry, soil strength parameters and the rupture distance ratio for the crescent failure is required. To date, there does not appear to be a satisfactory method for predicting the rupture distance ratio for 3-dimensional narrow tine soil failure. The rupture distance ratio model proposed by Hettiaratchi *et al.*,[3,6] whilst satisfactory for wide tines, gave errors up to 50% for narrow tines which was not sufficiently accurate to allow its use as a key factor in a force prediction model. It was therefore necessary to plot experimentally determined rupture distance ratios from the work of Payne,[4] Hettiaratchi *et al.*[6] and Payne and Tanner,[11] and results from the experimental work in this study against rake angle in *Fig. 11*. The results of the different studies are in

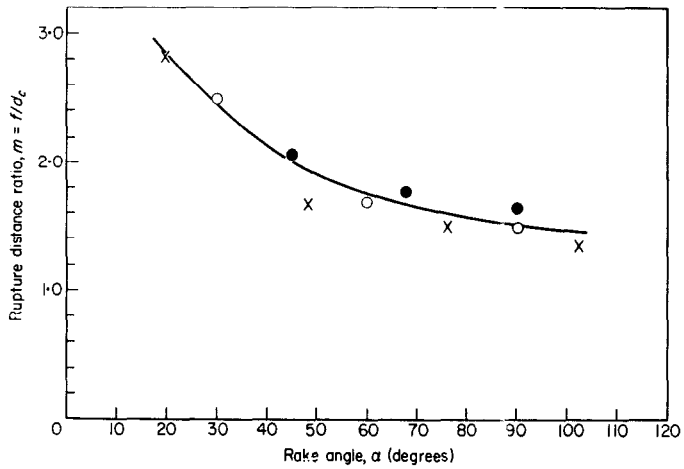

Fig. 11. Experimental relationship between rupture distance ratio and tine rake angle. ●, From Fig. 3; ○, from Hettiaratchi and Reece[6]; ×, from Payne[4] and Payne and Tanner[11]

close agreement. In the absence of a more rigorous prediction theory, the use of *Fig. 11* will allow reasonable estimates to be made of the rupture distance ratio for different rake angles. It should be noted that most of the data in *Fig. 11* was obtained from tests in soils having appreciable friction and density in addition to some cohesion. Little data is available on purely cohesive soils and on very loose frictional soils.

The main steps in the force calculation procedure can be summarized as follows.

1. Determine the rupture distance ratio for the particular rake angle from *Fig. 11*.
2. Determine N_γ, N_c, N_q, and N_a for the appropriate values of α, ϕ and δ from Hettiaratchi *et al.*[3] or from Hettiaratchi and Reece[14] which presents updated data (note N is referred to as K).
3. Determine N_c' and N_q' from *Fig. 8*.
4. Determine the depth of crescent failure of the tine from *Fig. 2* for compact frictional soils, or determine the critical depth using Eqn (20). N.B. If $d_c > d$ then all of the soil failure is of the crescent type.
5. Substitute into Eqns (19) and (13) for the horizontal and vertical force components, respectively.

6. Comparison of experimental and predicted tine forces

A series of tests was carried out in an experimental soil bin to determine the forces acting on a range of tines working under two different soil conditions. The forces and moments were

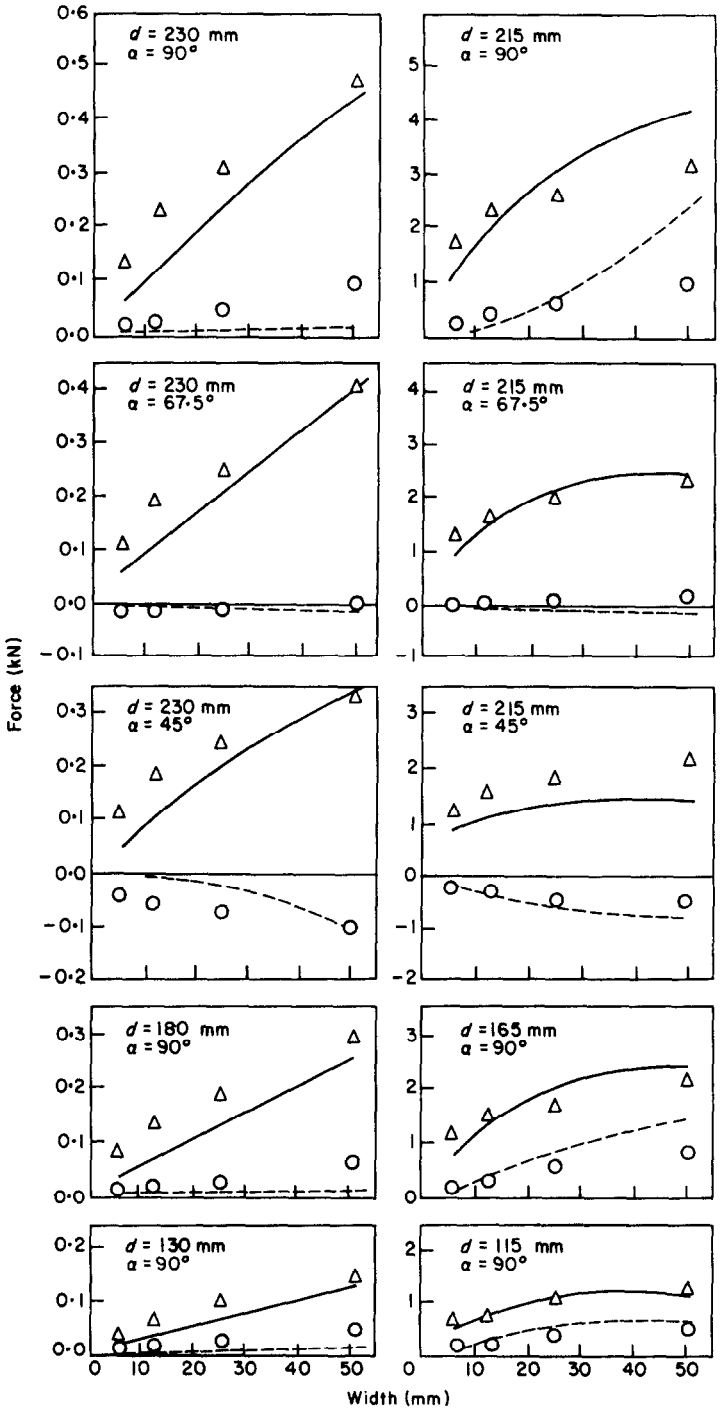

Fig. 12. Comparison between predicted and measured forces for a range of tine widths, in uncompacted soil (left) and compacted soil (right). ——, *Predicted horizontal force;* – – –, *predicted vertical force;* △, *measured horizontal force;* ○, *measured vertical force*

recorded using an extended octagonal ring transducer (Godwin[19]) and the tests were carried out at a forward speed of 0·56 m/s in a sandy loam soil. After each experimental run, the soil in the bin was loosened. The more dense soil was compacted to the required density by rolling 50 mm deep layers using a commercial pavement roller. Soil uniformity throughout the tests was monitored using a hand-held gamma-ray probe (Soane *et al.*[20]), a cone penetrometer and direct soil sampling.

The results from some of these tests on the soils described in sections 3 and 4, respectively, are shown in *Fig. 12*, together with the force predictions made using the minimizing prediction theory. The two soil conditions used, permitted the model to be evaluated for values of c and ϕ similar to those most frequently found for agricultural soils by Payne and Fountain.[21] These conditions were such that the forces on a particular tine were almost 10 times greater in the compacted soil than in the uncompacted soil. The general shape and order of magnitude of the predicted curves show reasonable agreement with the experimental data for the horizontal force component. For large aspect ratio tines, predictions are closer in the compacted soil than in the loose soil.

7. Conclusions

The tine force prediction model, based upon the observed soil failure pattern with narrow tines, has been shown to give useful agreement with experimental data for a range of tine geometries operating in two soil conditions. Both soil conditions had high angles of shearing resistance, but differed in density and cohesion. Generally the predictions were closest for the compact soil condition.

The critical depth can be estimated using a minimizing technique. This technique is useful for predicting the approximate critical depth at different soil densities. The model, however, is not sufficiently sensitive for precise predictions over a narrow range of soil densities and tine geometries.

Acknowledgements

The first author would like to express gratitude to Calor Agriculture for a Fellowship, during the tenure of which much of the work was conducted. The assistance given by D. G. Harris, J. Kilgour, G. Knowles, R. W. Sadler, F. G. Smith and Dr J. C. Taylor is gratefully acknowledged.

REFERENCES

[1] **Osman, M. S.** *The mechanics of soil cutting blades.* J. agric. Engng Res., 1964 **9** (4) 313–328

[2] **Siemens, J. C.; Weber, J. A.** *Soil bin and model studies on tillage tools and traction devices.* J. Terramech., 1964 **1** (2) 56–67

[3] **Hettiaratchi, D. R. P.; Witney, B. D.; Reece, A. R.** *The calculation of passive pressure in two-dimensional soil failure.* J. agric. Engng Res., 1966 **11** (2) 89–107

[4] **Payne, P. C. J.** *The relationship between the mechanical properties of soil and the performance of simple cultivation implements.* J. agric. Engng Res., 1956 **1** (1) 23–50

[5] **O'Callaghan, J. R.; Farrelly, K. M.** *Cleavage of soil by tined implements.* J. agric. Engng Res., 1964 **9** (3) 259–270

[6] **Hettiaratchi, D. R. P.; Reece, A. R.** *Symmetrical three-dimensional soil failure.* J. Terramech., 1967 **4** (3) 45–67

[7] **Zelenin, A. N.** *Fizicheski Osmovie Teorii Rezaniya Gruntov* (Basic physics of the theory of soil cutting). Moscow-Leningrad: Akademia Nawk USSR (N.I.A.E., Silsoe, Bedford, translation, un-numbered) 1950

[8] **Kostritsyn, A. K.** *Cutting of a cohesive medium with knives and cones.* N.I.A.E., Silsoe, Bedford, translation 58, 1956

[9] **Miller, P. C. H.** *Soil failure and the nature of the force system with very narrow tines.* Unpublished B.Sc. dissertation, National College of Agric. Engng, Silsoe, Bedford, 1971

[10] **O'Callaghan, J. R.; McCullen, P. J.** *Cleavage of soil by inclined and wedge-shaped tines.* J. agric. Engng Res., 1965 **10** (3) 248–254

[11] **Payne, P. C. J.; Tanner, D. W.** *The relationship between rake angle and the performance of simple cultivation implements.* J. agric. Engng Res., 1959 **4** (4) 312–325
[12] **Jaky, J.** *On the bearing capacity of piles.* Proc. 2nd Int. Conf. on Soil Mechanics and Foundation Engng, 1948
[13] **Meyerhof, G. C.** *The ultimate bearing capacity of foundations.* Geotechnique, 1951 **2** (4) 310–332
[14] **Hettiaratchi, D R. P.; Reece, A. R.** *The calculation of passive soil resistance.* Geotechnique, 1974 **24** (3) 289–310
[15] **Sokolovski, V. V.** *Statics of Soil Media.* London: Butterworth, 1956
[16] **Scott, R. F.** *Principles of Soil Mechanics.* Reading, Mass.: Addison-Wesley Publ. Co. Inc., 1963
[17] **Lambe, T. W.; Whitman, R. V.** *Soil Mechanics.* New York: John Wiley & Sons, Inc., 1969
[18] **Terzaghi, K.** *Theoretical Soil Mechanics.* New York: John Wiley & Sons, Inc., 1965
[19] **Godwin, R. J.** *An extended octagonal ring transducer for use in tillage studies.* J. agric. Engng Res., 1975 **20** (4) 347–352
[20] **Soane, B. D.; Campbell, D. J.; Herkes, S. M.** *Hand-held gamma-ray transmission equipment for the measurement of bulk density of field soils.* J. agric. Engng Res., 1971 **16** (2) 146–156
[21] **Payne, P. C. J.; Fountain, E. R.** *The mechanism of scouring for cultivation implements.* Tech. Memo. No. 116, N.I.A.E., Silsoe, Bedford, 1954